Electric Power Systems Research xxx (2014) xxx–xxx

Contents lists available at ScienceDirect

Electric Power Systems Research

journal homepage: www.elsevier.com/locate/epsr

Hierarchical automatic voltage control for integration of large-scale wind power: Design and implementation

Qinglai Guo, Hongbin Sun*, Bin Wang, Boming Zhang, Wenchuan Wu, Lei Tang

Department of Electrical Engineering, State Key Laboratory of Power Systems, Tsinghua University, Beijing 100084, China

ARTICLE INFO

Article history:
Available online xxx

Keywords:
Wind power integration
Automatic voltage control
Energy management system

ABSTRACT

Integration of high levels of wind power penetration is an important feature of the emerging smart transmission grid. To address the dramatic voltage fluctuations and wind turbine generators (WTGs) cascading trip faults, which have been greatly challenged the wind pool area's operation, a hierarchical automatic voltage control system to support wind power integration (Wind-AVC) is designed and presented in this paper. For each wind farm, an autonomous wind farm voltage controller (WFVC), which takes the details of the wind farm side grid into account, is applied to optimize the voltage and reactive power distribution inside the wind farm. Three different control modes are implemented to consider all the terminal voltages of WTGs as well as the dynamic Var reserves. A control center voltage controller (CCVC) is designed to coordinate all the distributed WFVCs. A security-constrained optimal power flow (SCOPF) based preventive control is presented, which ensures all the wind farms' voltage satisfying the operational constraints for all the possible $N-1$ scenarios. The Wind-AVC system has been put into operation in Northern China and was found to be effective in mitigating the voltage fluctuations and reducing the cascading trip risks.

1. Introduction

Accommodating greater levels of penetration of renewable energy sources is one of the most important features of smart grids. Wind energy is one of the most popular renewable energy sources, and significant wind power integration has already been achieved in electricity grids in a number of countries across the globe. Wind power can be integrated into distribution grids as distributed generators (DGs) or aggregated as large wind farms and connected to transmission grids. The latter approach accounts for the largest portion of the wind power generation in China, where the wind power capacity reached 76 GW at the end of 2012, which represents the largest scale integration of wind power in the world [1]. In China, there is a long-term plan to build seven or eight wind power bases with a minimum capacity of 10 GW each by 2020. However, many of the regions that this large-scale wind power integration is intended supply have relatively weak power grids. For example, in Zhangbei Wind Base, 18 wind farms are connected to the aggregation substation via a single 220 kV transmission line, where the power flow has reached 900 MW, approximately four times the surge impedance loading of the line. The short-circuit capacity in this area is also very small, so the voltage may change greatly in response to variations in the reactive power. During seasons when the wind is strong, switching a single 10 Mvar capacitor may lead to a voltage increase of more than 10 kV. Such an operation scheme, with large-scale wind power integration into a weak power grid, brings about considerable challenges for power system engineers.

The first challenge is related to the voltage fluctuations caused by the intermittent output of the wind turbine generators (WTGs) and the relatively weak grid structure. Historical data show that the voltage from the wind farms varies dramatically compared with conventional power generation. The range of fluctuation was more than 10% per day; for comparison, conventional substations typically fluctuate by less than 5% in a day. The rate of change in the voltage during these fluctuations may also be very rapid. In some wind farms, a fluctuation of more than 6 kV may occur within 10 s, and voltage variations of up to 5 kV have been observed to happen over only 2 s. Moreover, these fluctuations are determined by the intermittent nature of the wind, rendering them inherently irregular and unpredictable. For these reasons, conventional automatic voltage control (AVC) technology is not suitable for large-scale wind power integration, and so a modified approach is required.

The second challenge is how to improve the wind pool area's stability under disturbances. There have been a number of cascading trip-off failures in Northern and Northwest China involving

* Corresponding author. Tel.: +86 1062783086.
E-mail address: shb@tsinghua.edu.cn (H. Sun).

http://dx.doi.org/10.1016/j.epsr.2014.02.012
0378-7796/

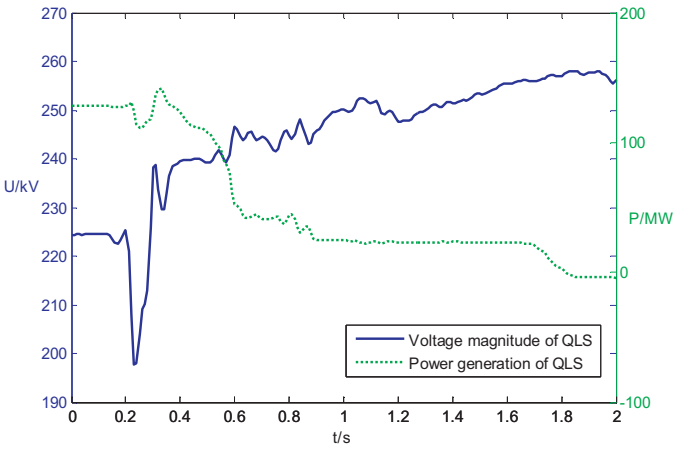

Fig. 1. Typical trip-off process voltage and power of a wind farm during a cascading failure.

thousands of WTGs. Investigations of these cascading faults have uncovered a commonality in the process [2–4]. First, all of these cascading faults occurred when the WTGs were operating at close to full capacity. The long transmission lines to transfer heavy wind power led to low voltage profiles in the area, which resulted in the capacitors in the wind farms and nearby substations being switched on to support the voltage. The cascading faults were triggered by short-circuit faults in one wind farm or substation, which caused the very low voltage. Unfortunately, most of the WTGs in China were not equipped with effective low-voltage ride through (LVRT) control that time, so these WTGs were shut down. Following the tripping of a large number of WTGs, the transmission line connected to the wind farm where the fault occurred changed from being heavily loaded to carrying a light load. Combined with the capacitors that were not switched off in time, this led to a sudden large amount of redundant reactive power. The wind power pool area was connected with a relatively weak power grid, which resulted in the voltage of the 220-kV transmission line reaching 245–255 kV. As a consequence, WTGs in other wind farms were tripped by the high-voltage protection. As more and more WTGs tripped, the voltage in this area became higher and higher, which resulted in even more WTGs being tripped off, i.e., a cascading failure occurred.

Fig. 1 shows the power and voltage generation from a wind farm named QLS during a typical cascading failure based on historical phasor measurement unit (PMU) data. We can divide the above cascading process into two phases. The first is the *trigger* phase, which starts when the fault occurs (just before 0.2 s) and ends when very low voltage occurs (just after 0.2 s). During this process, LVRT may improve the stability of the WTGs and provide reactive power support. Positive LVRT may avert a cascading failure before it starts. The second phase starts from the first tripping of the WTGs in the wind farm and ends with all the wind farms that are involved in the failure being tripped off. This is termed the *spreading* phase, during which the voltage increased considerably over a period of 2–3 s. During this phase, in addition to high voltage ride through (HVRT) technology to mitigate the voltage increase, a well-designed AVC technology, which will be discussed in this paper, is expected to be very useful.

AVC is one of the most important control systems employed in electrical power grids [5–7]. Many successful applications of this technology have been reported, with generally positive results [8–12]. In the emerging smart transmission grid [13], an AVC system supporting large-scale wind power integration (referred to hereafter as Wind-AVC) is urgently required to address the new challenges described above. Some researches [14–17] have been reported on this topic recently, covering WTG control, wind farm primary control and area secondary control. However, most of the current methods are still not satisfying the requirements of Chinese large wind bases with critical voltage fluctuations and high cascading trip risks. In this paper, Wind-AVC-related technologies will be discussed, and based on these technologies, a Wind-AVC system and its implementation in a large-scale wind pool area will be described.

The remainder of this paper is organized as follows. In Section 2, we will describe the distinct requirements regarding to the voltage control issues in a wind pool area. In Section 3, the architecture of a Wind-AVC system is designed and presented. The wind farm side and control center side technologies are described in Sections 4 and 5, respectively. Some results from field application are shown in Section 6. Finally, conclusions are drawn in Section 7.

2. Requirements for Wind-AVC

The particular demands of wind farms and wind power pool areas for Wind-AVC bring additional requirements compared with those of AVC for conventional power generation systems. The first is related to the control objectives. The controller inside a wind farm must maintain the terminal voltage of each WTG within certain limits (690 V ± 10% is typical), otherwise the WTG will be tripped by either low- or high-voltage protection. Unlike a conventional thermal or hydro power plant, a wind farm may be considered as a distribution grid connecting dozens of WTGs via several 35 kV feeders, which are often very long (more than 30 km in some cases in China). So the voltage drop along a feeder should not be neglected especially when heavy-loaded. For the two WTGs in the same feeder, which connect to the root node and the very end node respectively, the terminal voltage difference may be over 5% in some heavy-loaded cases. This means that, although the voltage of the root node may be nominal value, while the voltage on the end may already near the limitation and probably be tripped off because of a small disturbance. For this reason, the design of a wind farm-side voltage controller is much more complicated than that of a conventional power plant, as it must account for the voltage at dozens of WTGs along a number of feeders and consider the local network constraints.

The available control devices for Wind-AVC are also much more complicated than those of traditional AVC. For each wind farm, there are dozens of WTGs whose reactive powers can be online regulated. Besides, there may be shunt capacitors (or reactors) in the wind farms or integration substations. Furthermore, to prevent cascading failures, guidelines now require that most wind farms in China be equipped with SVCs (Static Var Compensator) or SVGs (Static Var Generator), which can provide dynamic reactive power support to compensate for disturbances. However, these fast compensators are not well coordinated with the relative slower ones (such as WTGs and shunt capacitors/reactors), in some cases, the fast-response Var is firstly exhausted during normal operation and therefore loses the dynamic response ability when disturbance occurs. The coordination of these reactive power regulators with different temporal response characteristics is another problem to be addressed.

The third requirement is the coordination of spatially distributed wind farms and substations. Many wind power pool areas are with relatively weak power grid, so the wind farms and substations that are connected together are strongly coupled. Disturbances (such WTGs being tripped) or control actions (such as switching a capacitor) in one wind farm will therefore significantly influence the voltage at other farms in the same region. This has been proved to be a major factor leading to WTGs cascading trip-off spreading from the first wind farm to others. So there should be a

Please cite this article in press as: Q. Guo, et al., Hierarchical automatic voltage control for integration of large-scale wind power: Design and implementation, Electr. Power Syst. Res. (2014), http://dx.doi.org/10.1016/j.epsr.2014.02.012

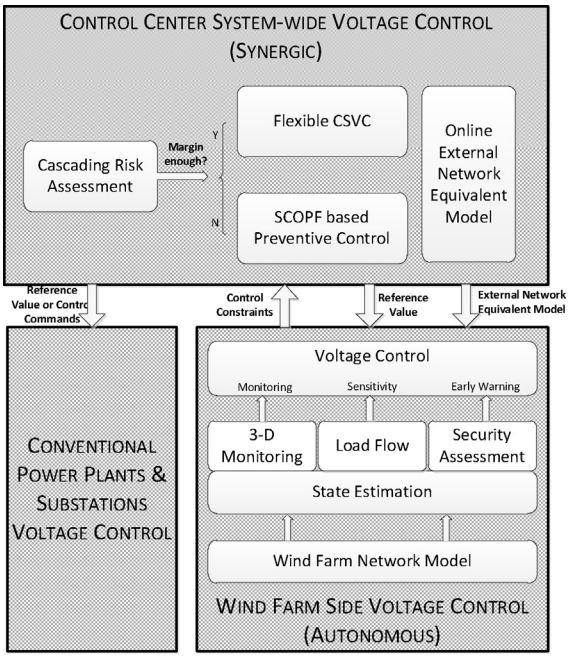

Fig. 2. Architecture of the implemented Wind-AVC system.

system-wide coordinator for the whole wind pool area to optimize all the wind farms and substations.

In a wind power pool area, there may be several dozens of wind farms with thousands of WTGs and hundreds of SVCs, SVGs, capacitors and/or reactors. It is unimaginable to find an area with such large amounts of control devices coupled together in a conventional power grid. Automatic voltage control to support large-scale wind power integration is therefore a new challenge for the emerging smart transmission grid.

3. Architecture

An autonomous-synergic Wind-AVC system is designed and implemented in China to meet the requirements proposed above. Fig. 2 shows the architecture of the Wind-AVC system, which has two-layer hierarchical structure. At the top level, a system-wide voltage controller is deployed in the control center, which is termed the control center voltage controller (CCVC). At the lower level, in addition to the conventional voltage controllers installed in conventional power plants and substations, a wind farm voltage controller (WFVC) is deployed in each wind farm.

The WFVC should coordinate the control devices (WTGs, SVCs, SVGs, capacitors and reactors) within a wind farm. To consider the detailed voltage profiles and Var distribution inside the wind farm, the WFVC was designed as a grid-model-based local voltage controller covering the whole wind farm grid. Such a system differs significantly from the conventional thermal or hydro power plant voltage controller. The accuracy of the WFCV calculation depends on the grid-model, including the internal radial grid inside the farm, which can be directly modeled by the WFVC, as well as the external network, which may vary in accordance with the topology and operational scheme of the whole power grid. This time-varying external network model, which describes the influence of the other parts of the power system when the WFVC makes local decision, is essential to ensure the autonomous feature of WFVC and is periodically generated and released online by the control center [18]. Based on the complete and independent network model that combines the internal and external ones, a set of advanced analysis modules is implemented in WFVC, including SE (state estimation), 3-D monitoring, LF (load flow), SA (security assessment) and VC (voltage control). In a sense, a WFVC, which covers modeling, analysis, assessment and close-loop control, can be considered a distributed energy management system (EMS) [19] for a single wind farm, which is why we define it as autonomous. Some details of the systems can be found in the preliminary paper [20], and the voltage control decision part will be proposed further in Section 4.

On the control center side, CCVC is implemented to coordinate all the autonomous WFVCs in the region as well as the local controllers within the conventional power plants and substations. According to the current controllable capacity of the SVGs, SVCs, WTGs and shunt capacitors, the WFVC online calculates the Var regulating ability and sends it to the control center as constraints. In CCVC, all the Var control devices within a wind farm are aggregated into a single-machine model with the regulating constraints determined by the farm itself. The control objective of the CCVC is to achieve optimal voltage and Var distribution satisfying the operation constraints, and its outputs include the reference values of the high-side voltage for WFVCs as well as conventional power plants, and control commands to directly switch on/off shunt capacitors/reactors in the conventional substations. The risk of cascading failures is assessed periodically to check if the security margin is sufficient. If it is, the CCVC is set to a CSVC (coordinated secondary voltage control) mode, the details of which can be found in Ref. [11]. Otherwise, CCVC will be switched to a preventive control mode, which is based on a SCOPF (security-constrained optimal power flow) model. In CSVC mode, only the current operation constraints are considered, while in SCOPF-based preventive control mode, $N-1$ contingency constraints are also included to ensure that the voltage of the wind farms satisfy the operational limits not only in base-case but also in all the possible $N-1$ scenarios. Preventive control is to get synergic effects to keep the wind pool area safe even under potential cascading faults, and the details will be discussed in Section 5.

4. Autonomous voltage control in WFVC

The kernel of WFVC is the voltage control strategy calculation, which outputs the regulation commands for all the WTGs, SVC/SVGs and shunt capacitors. Three control modes were designed for different operating requirements ranked by the priority: (a) corrective control mode, which aims to maintain all the WTGs' terminal voltage within limits; (b) coordinated control mode, which aims to follow a reference value sent from control center and mitigate the voltage fluctuations considering all necessary operation constraints; (c) preventive control mode, which substitutes the dynamic reactive power reserve with other slower Var sources, on the premise of keeping both the WTGs' terminal voltages and the high-side voltage within the required threshold. The detailed models of the three modes will be presented in the following sections (Fig. 3).

The outputs are the set-points and action commands for the reactive power regulation devices. Series of improvements on the Var regulators in the wind farm have been carried out according to the investigation suggestions for the cascading issues. First of all, the WTG, which once did not support online regulation of its Var outputs, has now been able to track the Var set-point by upgrading the converters with constant-Q control loop. It is essential for the voltage control because the number of WTGs is considerable. Furthermore, the WTGs are distributed along the feeders so it becomes possible to control the voltages on different nodes all over the wind farm grid, rather than merely changing the root voltage by controlling the capacitors or SVCs in the past.

Secondly, for SVCs/SVGs, both constant-V and constant-Q control are optional. We should choose constant-V control if we

Please cite this article in press as: Q. Guo, et al., Hierarchical automatic voltage control for integration of large-scale wind power: Design and implementation, Electr. Power Syst. Res. (2014), http://dx.doi.org/10.1016/j.epsr.2014.02.012

suppose SVCs/SVGs to offer dynamic Var support during disturbances. However, considering that the WTGs are working with constant-Q mode, the SVCs/SVGs, if adopting constant-Q mode, will be much easier to be coordinated with WTGs. So a new control algorithm combining the constant-V and constant-Q modes has been designed and developed for SVCs/SVGs. For the SVC i (SVG is just the same), the WFVC will output a pair of set-points as $\left(\left[\underline{V}_{svc_i}^{ref}, \bar{V}_{svc_i}^{ref}\right], Q_{svc_i}^{ref}\right)$. Here, y is a voltage limits within which the SVC must maintain its terminal voltage. If the SVC's terminal voltage violates this range, it will regulate the Var output to pull the voltage back in several milliseconds. So the SVCs will still retain the dynamic voltage support capability to against disturbances. When $\left[\underline{V}_{svc_i}^{ref}, \bar{V}_{svc_i}^{ref}\right]$ is satisfied, the SVC will enter the constant-Q mode and track $Q_{svc_i}^{ref}$. In this way the SVC can be coordinated with the WTGs effectively.

As discussed in the previous section, the capacitors are proved to have taken negative effect during the cascading failure. Therefore, in WFVC, the capacitors are the last considered devices that will only be switched on when all the WTGs and SVCs/SVGs have reached the upper limit while the voltage is still violating the lower limit.

The detailed model for the three modes will be discussed in the following subsections.

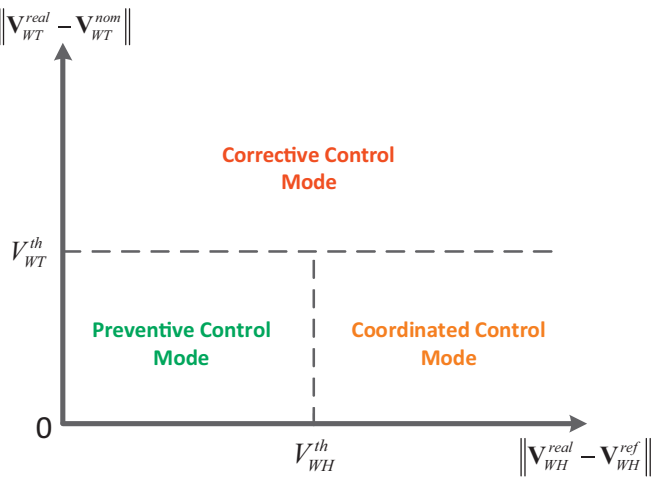

Fig. 3. Three voltage control modes for WFVC. The x-axis is the bias of the high-side voltage, and the y-axis is the difference between the terminal voltage of the WTGs and the nominal value.

4.1. Corrective voltage control mode

If $\left\|\boldsymbol{V}_{WT}^{real} - \boldsymbol{V}_{WT}^{nom}\right\| \geq V_{WT}^{th}$, the WFVC will switch to the corrective control mode. Here, $\boldsymbol{V}_{WT}^{real} = [V_{wt,1}^{real}, \ldots, V_{wt,n_w}^{real}]^T$, where $V_{wt,i}^{real}$ is the real-time magnitude value of the terminal voltage of WTG i and n_w is the number of WTGs in the wind farm. $\boldsymbol{V}_{WT}^{nom}$ is a vector describing the nominal terminal voltage for each WTG (typically 1.0 p.u.). V_{WT}^{th} refers to the threshold value, which can be selected as 0.1 p.u. as the protection configuration usually is [0.9 p.u., 1.1 p.u.]. However, to ensure sufficient operation margins, V_{WT}^{th} is usually configured as 0.07–0.08 p.u. in the real-life implementation.

The corrective control mode model is as follows:

$$\begin{aligned}
&\min_{\Delta\boldsymbol{Q}_{WT},\Delta\boldsymbol{Q}_S} W_T\left\|\boldsymbol{V}_{WT}^{real} - \boldsymbol{V}_{WT}^{nom} + \boldsymbol{C}_{TW}\Delta\boldsymbol{Q}_{WT} + \boldsymbol{C}_{TS}\Delta\boldsymbol{Q}_S\right\|^2 \\
&\quad + W_W\left\|\Delta\boldsymbol{Q}_{WT}\right\|^2 + W_S\left\|\Delta\boldsymbol{Q}_S\right\|^2 \\
&\text{s.t.} \quad \boldsymbol{V}_{WT}^{\min} \leq \boldsymbol{V}_{WT}^{real} + \boldsymbol{C}_{TW}\Delta\boldsymbol{Q}_{WT} + \boldsymbol{C}_{TS}\Delta\boldsymbol{Q}_S \leq \boldsymbol{V}_{WT}^{\max} \\
&\boldsymbol{V}_S^{\min} \leq \boldsymbol{V}_S^{real} + \boldsymbol{C}_{SW}\Delta\boldsymbol{Q}_{WT} + \boldsymbol{C}_{SS}\Delta\boldsymbol{Q}_S \leq \boldsymbol{V}_S^{\max} \\
&\boldsymbol{V}_{WH}^{\min} \leq \boldsymbol{V}_{WH}^{real} + \boldsymbol{C}_{HW}\Delta\boldsymbol{Q}_{WT} + \boldsymbol{C}_{HS}\Delta\boldsymbol{Q}_S \leq \boldsymbol{V}_{WH}^{\max} \\
&\boldsymbol{Q}_{WT}^{\min} \leq \boldsymbol{Q}_{WT} + \Delta\boldsymbol{Q}_{WT} \leq \boldsymbol{Q}_{WT}^{\max} \\
&\boldsymbol{Q}_S^{\min} \leq \boldsymbol{Q}_S + \Delta\boldsymbol{Q}_S \leq \boldsymbol{Q}_S^{\max}
\end{aligned} \tag{1}$$

where $\Delta\boldsymbol{Q}_{WT}$ and $\Delta\boldsymbol{Q}_S$ are the Var regulation vector of the WTGs and SVCs/SVGs, respectively, which are to be optimized. $\boldsymbol{C}_{TW}$ and $\boldsymbol{C}_{TS}$ are the sensitivity matrices for the WTGs' terminal voltage $\boldsymbol{V}_{WT}$ w.r.t. $\Delta\boldsymbol{Q}_{WT}$ and $\Delta\boldsymbol{Q}_S$. $\boldsymbol{C}_{SW}$ and $\boldsymbol{C}_{SS}$ denote the sensitivity matrix for the SVCs/SVGs' terminal voltage $\boldsymbol{V}_S$ w.r.t. $\Delta\boldsymbol{Q}_{WT}$ and $\Delta\boldsymbol{Q}_S$. $\boldsymbol{C}_{HW}$ and $\boldsymbol{C}_{HS}$ denote the sensitivity matrices for the wind farm's high-side voltage $\boldsymbol{V}_{WH}$ w.r.t. $\Delta\boldsymbol{Q}_{WT}$ and $\Delta\boldsymbol{Q}_S$. The superscript *real* refers to the current real-time value sampled by the controller. $\boldsymbol{V}_{WT}^{\min}$, $\boldsymbol{V}_{WT}^{\max}$, $\boldsymbol{V}_S^{\min}$, $\boldsymbol{V}_S^{\max}$, $\boldsymbol{V}_{WH}^{\min}$, $\boldsymbol{V}_{WH}^{\max}$, $\boldsymbol{Q}_{WT}^{\min}$, $\boldsymbol{Q}_{WT}^{\max}$, $\boldsymbol{Q}_S^{\min}$ and $\boldsymbol{Q}_S^{\max}$ are the operating limits for $\boldsymbol{V}_{WT}$, $\boldsymbol{V}_S$, $\boldsymbol{V}_{WH}$, $\boldsymbol{Q}_{WT}$ and $\boldsymbol{Q}_S$, respectively, and we have $V_{WT,i}^{\min} = V_{WT,i}^{nom} - V_{WT}^{th}$ and $V_{WT,i}^{\max} = V_{WT,i}^{nom} + V_{WT}^{th}$. W_T, W_W and W_S are weighting coefficients. Corrective control is to find optimal solutions $\Delta\boldsymbol{Q}_{WT}^*$ and $\Delta\boldsymbol{Q}_S^*$ to ensure that all the terminal voltages remains within the limitations, as well as satisfying other operating constraints.

4.2. Coordinated voltage control mode

If $\left\|\boldsymbol{V}_{WT}^{real} - \boldsymbol{V}_{WT}^{nom}\right\| < V_{WT}^{th}$ and $\left\|\boldsymbol{V}_{WH}^{real} - \boldsymbol{V}_{WH}^{ref}\right\| \geq V_{WH}^{th}$, the WFVC will switch to the coordinated control mode. In this situation, all the terminal voltages of WTGs satisfy the operating constraints, but the bias of the high-side voltage $\boldsymbol{V}_{WH}^{real}$ and its reference value, $\boldsymbol{V}_{WH}^{ref}$, which is got from the control center periodically, violates the allowed dead band V_{WH}^{th}. In general, if the high-side voltage of the wind farm is 220 kV, then V_{WH}^{th} is usually set as 1.0 kV.

Coordinated voltage control is designed to track the reference value updated by CCVC satisfying the operating constrains. Its model is as the follows:

$$\begin{aligned}
&\min_{\Delta\boldsymbol{Q}_{WT},\Delta\boldsymbol{Q}_S} W_H\left\|\boldsymbol{V}_{WH}^{real} - \boldsymbol{V}_{WH}^{ref} + \boldsymbol{C}_{HW}\Delta\boldsymbol{Q}_{WT} + \boldsymbol{C}_{HS}\Delta\boldsymbol{Q}_S\right\|^2 \\
&\quad + W_W\left\|\Delta\boldsymbol{Q}_{WT}\right\|^2 + W_S\left\|\Delta\boldsymbol{Q}_S\right\|^2 \\
&\text{s.t.} \quad \boldsymbol{V}_{WT}^{\min} \leq \boldsymbol{V}_{WT}^{real} + \boldsymbol{C}_{TW}\Delta\boldsymbol{Q}_{WT} + \boldsymbol{C}_{TS}\Delta\boldsymbol{Q}_S \leq \boldsymbol{V}_{WT}^{\max} \\
&\boldsymbol{V}_S^{\min} \leq \boldsymbol{V}_S^{real} + \boldsymbol{C}_{SW}\Delta\boldsymbol{Q}_{WT} + \boldsymbol{C}_{SS}\Delta\boldsymbol{Q}_S \leq \boldsymbol{V}_S^{\max} \\
&\boldsymbol{V}_{WH}^{\min} \leq \boldsymbol{V}_{WH}^{real} + \boldsymbol{C}_{HW}\Delta\boldsymbol{Q}_{WT} + \boldsymbol{C}_{HS}\Delta\boldsymbol{Q}_S \leq \boldsymbol{V}_{WH}^{\max} \\
&\boldsymbol{Q}_{WT}^{\min} \leq \boldsymbol{Q}_{WT} + \Delta\boldsymbol{Q}_{WT} \leq \boldsymbol{Q}_{WT}^{\max} \\
&\boldsymbol{Q}_S^{\min} \leq \boldsymbol{Q}_S + \Delta\boldsymbol{Q}_S \leq \boldsymbol{Q}_S^{\max}
\end{aligned} \tag{2}$$

The constrains in (2) is just the same as the corrective control model (1), while the objective function here is designed to follow the reference value $\boldsymbol{V}_{WH}^{ref}$ as well as to minimize the control cost. W_H, W_W and W_S are weighting coefficients.

4.3. Preventive voltage control mode

When $\left\|\boldsymbol{V}_{WT}^{real} - \boldsymbol{V}_{WT}^{nom}\right\| < V_{WT}^{th}$ and $\left\|\boldsymbol{V}_{WH}^{real} - \boldsymbol{V}_{WH}^{ref}\right\| < V_{WH}^{th}$, the preventive control as (3) will be carried out to maximize the dynamic Var reserves.

Please cite this article in press as: Q. Guo, et al., Hierarchical automatic voltage control for integration of large-scale wind power: Design and implementation, Electr. Power Syst. Res. (2014), http://dx.doi.org/10.1016/j.epsr.2014.02.012

$$\begin{aligned}
&\min_{\Delta \boldsymbol{Q}_{WT}} W'_S \left\| \boldsymbol{Q}_S + \Delta \boldsymbol{Q}_S - \frac{1}{2}(\boldsymbol{Q}_s^{\max} - \boldsymbol{Q}_s^{\min}) \right\|^2 + W'_W \left\| \Delta \boldsymbol{Q}_{WT} \right\|^2 \\
&\text{s.t.} \quad \boldsymbol{V}_{WT}^{\min} \le \boldsymbol{V}_{WT}^{real} + \boldsymbol{C}_{TW} \Delta \boldsymbol{Q}_{WT} + \boldsymbol{C}_{TS} \Delta \boldsymbol{Q}_S \le \boldsymbol{V}_{WT}^{\max} \\
&\underline{\boldsymbol{V}}_{WH}^{ref} \le \boldsymbol{V}_{WH}^{real} + \boldsymbol{C}_{HW} \Delta \boldsymbol{Q}_{WT} + \boldsymbol{C}_{HS} \Delta \boldsymbol{Q}_S \le \bar{\boldsymbol{V}}_{WH}^{ref} \\
&\boldsymbol{Q}_{WT}^{\min} \le \boldsymbol{Q}_{WT} + \Delta \boldsymbol{Q}_{WT} \le \boldsymbol{Q}_{WT}^{\max} \\
&\boldsymbol{Q}_S^{\min} \le \boldsymbol{Q}_S + \Delta \boldsymbol{Q}_S \le \boldsymbol{Q}_S^{\max} \\
&\boldsymbol{C}_{SS} \Delta \boldsymbol{Q}_S + \boldsymbol{C}_{SW} \Delta \boldsymbol{Q}_{WT} = 0
\end{aligned} \tag{3}$$

In corrective or coordinated control modes, the reference values of the SVCs/SVGs updated by the WFVC are as $\left(\left[V_{S,i}^{\min}, V_{S,i}^{\max} \right], Q_{S,i}^{ref} \right)$. Since the terminal voltage limitation of the SVC/SVG is adopted as in its reference, unless some disturbance occurs, or the SVC/SVG will simply follow the Var reference $Q_{S,i}^{ref}$. So the SVCs/SVGs are mainly working with constant-Q mode. However, in preventive control mode, the voltage reference of the ith SVC/SVG from the WFVC is $\left[V_{S,i}^{real} - \xi, \quad V_{S,i}^{real} + \xi \right]$, where ξ is a small deviation. So the SVC/SVG is supposed to work with constant-V mode and maintain the voltage at $V_{S,i}^{real}$. In Eq. (3), the control variable is $\Delta \boldsymbol{Q}_{WT}$ only, and a new constraint $\boldsymbol{C}_{SS} \Delta \boldsymbol{Q}_S + \boldsymbol{C}_{SW} \Delta \boldsymbol{Q}_{WT} = 0$ is added to describe the quasi-steady-state response of SVCs/SVGs' constant-V control, from which the $\Delta \boldsymbol{Q}_S$ can be estimated by assuming that $\boldsymbol{V}_S$ remains constant. Another difference in the constraints is that the high-side voltage should be maintained in the threshold $\left[\underline{\boldsymbol{V}}_{WH}^{ref}, \bar{\boldsymbol{V}}_{WH}^{ref} \right]$ (i.e., around $\boldsymbol{V}_{WH}^{ref}$), rather than the original operation limits $\left[\boldsymbol{V}_{WH}^{\min}, \boldsymbol{V}_{WH}^{\max} \right]$. These constraints require that preventive control should be carried out without affecting the high-side voltage.

The objective of (3) is to maximize the dynamic Var reserve of SVCs/SVGs by driving their Var output to the middle, so there will be the largest capacities for both upward and downward regulation. Here, W'_S and W'_W are weighting coefficients, and the former has the higher priority.

5. Synergic voltage control in CCVC

The major novel aspect of CCVC is the SCOPF-based preventive control method. As discussed in Section 1, cascading failures typically occur within 2–3 s. Once triggered, there is very little time to take effective control measures. It is therefore highly desirable to implement system-wide preventive control to ensure that the wind power pool area functions within normal operating conditions even when contingencies occur. In conventional system-wide voltage control strategies such as CSVC, only the current operating constraints are considered. The system may be held in a status that satisfies all the operating constraints, which we define it as the *normal* state. However, once a contingency happens, for instance, when a wind farm or a transmission line is out of operation because of fault, the reminder of the grid may not be able to still satisfy the operating constraints. We consider this not to be *safe*. In a cascading failure, prior to the fault, the wind power pool area was actually working in a *normal but not safe* state, which means that a localized fault may lead to voltage violations at other wind farms, and ultimately induce a cascading outage. Via preventive control, the system is optimized so that it should always operate in a *normal and safe* state, which not only satisfies all the current operating limitations but is also without violations under all the potential post-contingency scenarios. The SCOPF-based model can achieve system-wide preventive control, as described by

$$\begin{aligned}
&\min_{u^0} \quad f(x^0, u^0) && \text{(a)} \\
&\text{s.t.} \quad g_0(x^0, u^0) = 0 && \text{(b)} \\
&\qquad g_k(x^k, u^0) = 0 && \text{(c)} \\
&\qquad \underline{x} \le x^0 \le \bar{x} && \text{(d)} \\
&\qquad \underline{x}^k \le x^k \le \bar{x}^k && \text{(e)} \\
&\qquad \underline{u} \le u^0 \le \bar{u} && \text{(f)} \\
&\qquad k = 1, \ldots, N_C
\end{aligned} \tag{4}$$

where x denotes the state variables (voltage magnitude V_i and voltage phase angle θ_i for node i), and u denotes the control variables. The superscript k refers to the value under the kth contingency and $k = 0$ refers to the pre-contingency base-case. N_C is the number of contingencies to be considered. Function $g(x, u) = 0$ is the load flow equation. The SCOPF model seeks an optimized control u^0 satisfying the constraints (4-f). u^0 will be performed on the base-case and maintained unchanged when the kth contingency occurs. So through constraints (4-b) and (4-c), we can calculate the states of the base-case x^0 and x^k under the kth post-contingency condition, which are required to satisfy the operation constraints (4-d) and (4-e). If both the base-case constraints ((4-b) and (4-d)) and the post-contingency constraints under all the pre-defined contingencies ((4-c) and (4-e)) are satisfied, then x^0 could be regarded as *normal and safe*. Within all the feasible solutions, u^0 with the minimum objective value is the final optimized solution.

Here u_0 includes $\{\boldsymbol{Q}_w^0, \boldsymbol{Q}_g^0, \boldsymbol{P}_w^0\}$, where $\boldsymbol{P}_w^0$ and $\boldsymbol{Q}_w^0$ are the active and reactive power outputs of the wind farms, respectively, and $\boldsymbol{Q}_g^0$ refers to the reactive power output of the conventional generators and compensators in the same area. The objective function is then

$$\min_{\left\{ \boldsymbol{Q}_w^0, \boldsymbol{Q}_g^0, \boldsymbol{P}_w^0 \right\}} \quad -w_1 f_1 + w_2 f_2 \tag{5}$$

where

$$f_1 = \sum_{i=1}^{N_w} P_{w,i}^0 \tag{6}$$

$$f_2 = P_{Loss} = \sum_{(i,j) \in NL} (P_{ij} + P_{ji}) \tag{7}$$

There are two parts in the objective function: the first part with the higher-priority weighting w_1 is to maximize the MW output of all the N_w wind farms; the second part, with lower-priority weight w_2, represents transmission losses, where P_{ij} and P_{ji} denote the active power of the branch (i, j) on the start node i and the end node j, respectively. NL refers to the set of the branches.

In this paper, the contingencies to be considered are the $N-1$ of the wind farms. Suppose there are N_w wind farms in the area, the kth wind farm $N-1$ is described as:

$$\begin{cases}
P_{w,i}^k = 0 & i = k \\
P_{w,i}^k = P_{w,i}^0 & i \ne k \\
Q_{w,i}^k = 0 & i = k \\
Q_{w,i}^k = Q_{w,i}^0 & i \ne k
\end{cases} \quad i = 1, \ldots, N_w \tag{8}$$

For (4-d) and (4-e), we are most concerned with the voltage magnitude limitations, especially the wind farms' voltage that should be limited to avoid the WTGs being tripped off on base-case as well as the $N-1$ contingencies.

Note that the active power outputs of wind farms, $\boldsymbol{P}_w^0$, is also included in the optimization together with the reactive power outputs. In some cases, optimizing only $\boldsymbol{Q}_w^0$ and $\boldsymbol{Q}_g^0$ may not be sufficient to find a feasible solution to satisfy all of the pre- and

Please cite this article in press as: Q. Guo, et al., Hierarchical automatic voltage control for integration of large-scale wind power: Design and implementation, Electr. Power Syst. Res. (2014), http://dx.doi.org/10.1016/j.epsr.2014.02.012

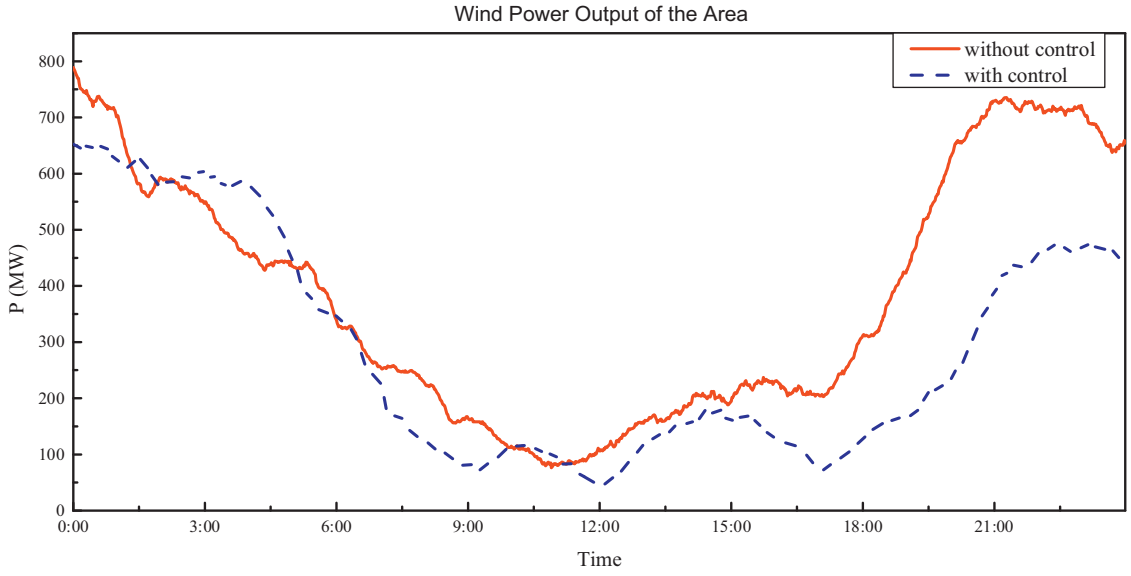

Fig. 4. Wind power output before and after the implementation of Wind-AVC. The solid red curve shows the active power on 13 November 2011 without Wind-AVC. The blue dashed curve shows the active power on 18 October 2012 following the implementation of Wind-AVC.

post-contingency constraints. So $\boldsymbol{P}_w^0$ must be curtailed. For this reason, f_1 is modeled in the objective function to maximize the wind farms' active power outputs to accommodate as much wind power as possible, of course, in the premise of ensuring the safe operation both on pre- and post-contingency situations.

The SCOPF-based model is considerably more complicated than the conventional OPF, for the constraints of SCOPF are nearly $N_C + 1$ times than that of a traditional OPF. A Benders decomposition based method [21] is adopted to solve Eq. (4), where the $N_C + 1$ contingencies (including the pre-contingency base-case) are formed as sub-problems, respectively. According to the optimized u^0, the reference value for the wind farms could be calculated and released to the WFVCs.

6. Field application results

The Wind-AVC system designed and developed by this paper was implemented in Zhangbei Wind Power Base of Northern China. Until July of 2013, 24 wind farms, including 1589 WTGs with the total generating capacity of 2379 MW, and 50 SVCs/SVGs with the total regulation capacity of ±1000 Mvar, have been closed-loop controlled by the Wind-AVC system. Some results from real-life application are shown in the Section.

To evaluate the control performance of the close-loop control system, 2 days with similar operating conditions [11] and wind power generation, as shown in Fig. 4, were selected to be compared. Considering the intermittent characteristics, it is difficult to find 2

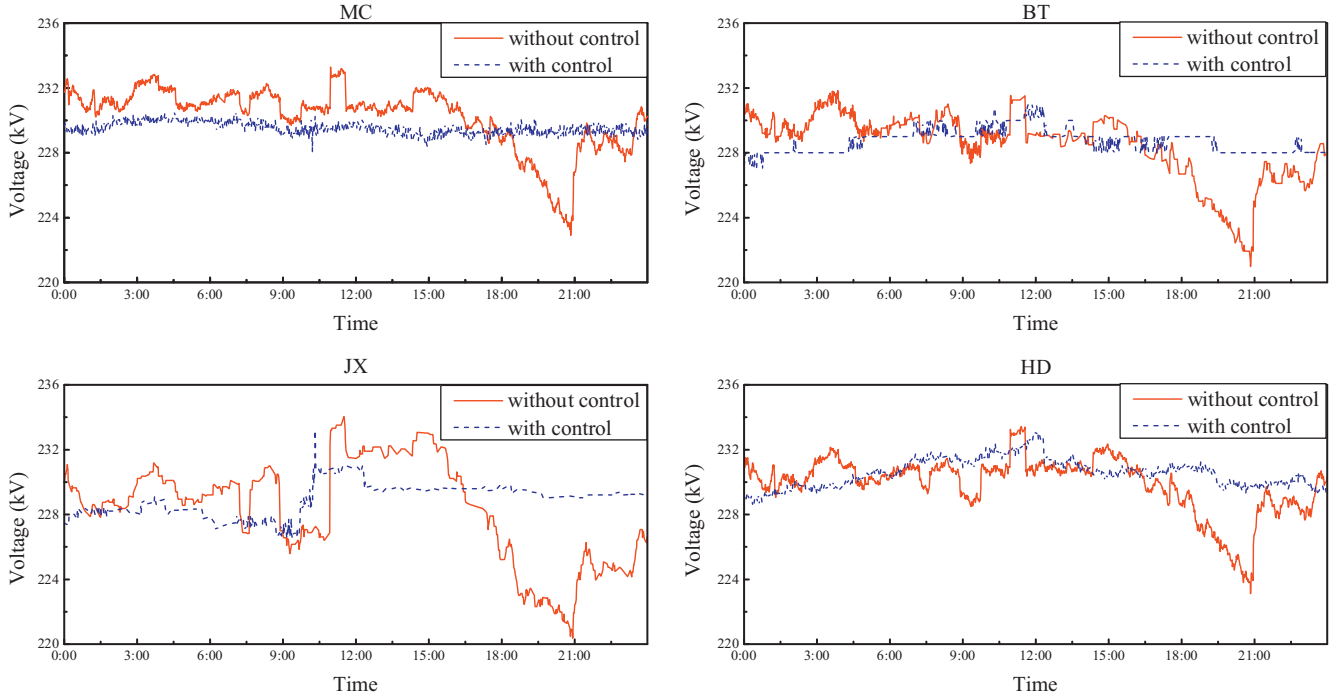

Fig. 5. Voltage curves comparison of typical wind farms with and without Wind-AVC.

Please cite this article in press as: Q. Guo, et al., Hierarchical automatic voltage control for integration of large-scale wind power: Design and implementation, Electr. Power Syst. Res. (2014), http://dx.doi.org/10.1016/j.epsr.2014.02.012

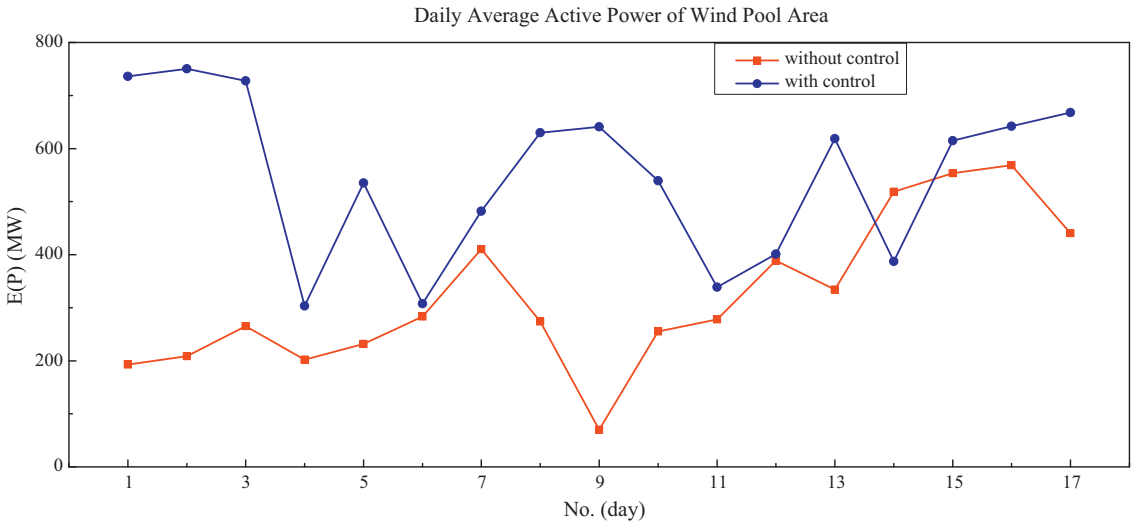

Fig. 6. The daily average active power of the wind power pool area over a 17-day period with and without Wind-AVC.

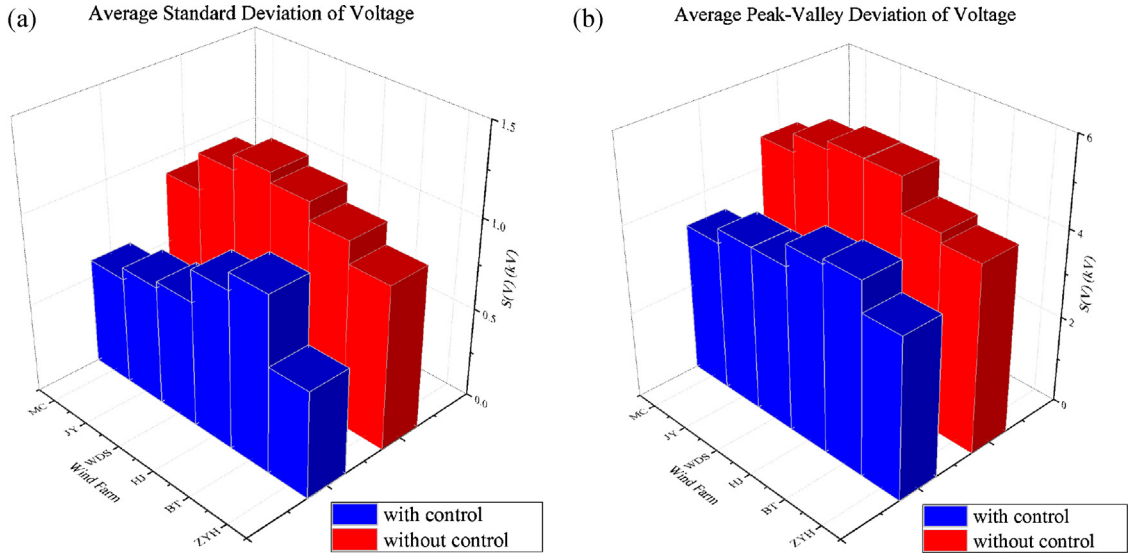

Fig. 7. Voltage fluctuation comparison of the wind pool area for long-term test with and without Wind-AVC.

days with identical wind power output. As shown in Fig. 4, the two days' wind power were very similar before 15:00, whereas later, the day without control was with higher wind power output than the day with control, however, they were still with a similar trend.

Fig. 5 shows the comparison of the high-side voltage of several typical wind farms in the area. It is clear that the voltage fluctuation was greatly reduced thanks to the Wind-AVC. The voltage profiles with control were much smoother, especially when the wind power rose rapidly shortly after noon, some very sharp voltage drops were observed on the day without Wind-AVC, while in contrast, the voltage could still be kept flat and smooth with Wind-AVC.

Long-term comparison was also carried out, in which we selected two half-months. The first was from August 1st to 17th, 2012, when the wind area was during the low-wind season prior to the implementation of Wind-AVC, and the second was from October 15th to 31st, 2012, when the wind area was during the

Table 1
Voltage fluctuation comparison of the wind farms for long-term test with and without AVC.

Wind farms	Average standard deviation			Average peak-valley deviation		
	Without control (kV)	With control (kV)	Reduction (%)	Without control (kV)	With control (kV)	Reduction (%)
ZYH	0.91	0.59	34.70	4.28	3.67	14.18
BT	1.03	0.97	5.63	4.50	4.35	3.17
HJ	1.13	0.87	22.47	5.28	4.24	19.60
WDS	1.18	0.70	41.13	5.29	3.75	29.03
JY	1.10	0.66	39.88	5.11	3.75	26.60
MC	0.90	0.60	33.59	4.70	3.42	27.26

Please cite this article in press as: Q. Guo, et al., Hierarchical automatic voltage control for integration of large-scale wind power: Design and implementation, Electr. Power Syst. Res. (2014), http://dx.doi.org/10.1016/j.epsr.2014.02.012

strong-wind season and the Wind-AVC was closed-loop controlled. The daily average wind power output comparison is shown as Fig. 6. Note that the wind power outputs of the days with Wind-AVC were obviously much higher than that of the days without control. This means that, it is likely that control was more challenging due to the greater wind power generated. However, as shown in Fig. 7 and Table 1, the voltage fluctuations had a smaller average standard deviation as well as lower peak-to-valley deviation with the closed-loop control of Wind-AVC.

Importantly, thanks to the autonomous-synergy voltage control scheme, the voltage distributions in the wind pool area are more reasonable and the cascading trip risk is also reduced. The Wind-AVC system is proved to be one of the important reasons to improve the operation security and reliability.

7. Conclusions

The necessities and challenges of AVC techniques to support large-scale wind power integration are discussed in this paper. A hierarchical Wind-AVC system has been researched and implemented, which main contributions include:

(1) The detailed model of the grid inside a wind farm is considered in the wind farm autonomous voltage controller. Not only the root voltage, but also all the terminal voltages of WTGs as well as the dynamic Var reserves are taken into account. The voltage fluctuations have been greatly mitigated.
(2) On the system side, a SCOPF-based preventive control, which considers not only the base-case but also the $N-1$ post-contingency performances, is presented to mitigate the cascading trip risk of the wind pool areas.

The real-life application results have proven a positive effect. Future research is ongoing to consider the wind power forecasting information into the control strategies.

Acknowledgements

This work was supported in part by the National Key Basic Research Program of China (973 Program) (2013CB228206), the National Science Fund for Distinguished Young Scholars (51025725), National Science Foundation of China (51277105 and 51321005) and Beijing Higher Education Young Elite Teacher Project (YETP0096).

References

[1] http://en.wikipedia.org/wiki/Wind_power_in_the_People's_Republic_of_China
[2] G. Mu, J. Wang, G. Yan, Cascading trip-off of doubly-fed induction generators from grid at near full-load condition in a wind farm, Automation of Electric Power Systems 35 (22) (2011) 35–40.
[3] D. Li, L. Jia, X. Xu, et al., Cause and countermeasure analysis on wind turbines' trip-off from grid, Automation of Electric Power Systems 35 (22) (2011) 41–44.
[4] X. Ye, Z. Lu, Y. Qiao, et al., A primary analysis on mechanism of large scale cascading trip-off of wind turbine generators, Automation of Electric Power Systems 36 (8) (2012) 35–40.
[5] J.P. Paul, J.Y. Leost, J.M. Tesseron, Survey of the secondary voltage control in France: present realization and investigations, IEEE Transactions on Power Systems 2 (May) (1987) 505–511.
[6] M. Ilic-Spong, J. Christensen, K.L. Eichorn, Secondary voltage control using pilot point information, IEEE Transactions on Power Systems 3 (May (2)) (1988) 660–668.
[7] P. Lagonotte, J.C. Sabonnadiere, J.Y. Leost, J.P. Paul, Structural analysis of the electrical system: application to secondary voltage control in France, IEEE Transactions on Power Systems 4 (May (2)) (1989) 479–486.
[8] H. Lefebvre, D. Fragnier, J.Y. Boussion, P. Mallet, M. Bulot, Secondary coordinated voltage control system: feedback of EDF, in: Proc. IEEE Power Engineering Society Summer Meeting, 2000, pp. 290–295.
[9] S. Corsi, M. Pozzi, C. Sabelli, A. Serrani, The coordinated automatic voltage control of the Italian transmission grid – Part I: reasons of the choice and overview of the consolidated hierarchical system, IEEE Transactions on Power Systems 19 (November (4)) (2004) 1723–1732.
[10] S. Corsi, M. Pozzi, M. Sforna, G. Dell'Olio, The coordinated automatic voltage control of the Italian transmission grid – Part II: control apparatuses and field performance of the consolidated hierarchical system, IEEE Transactions on Power Systems 19 (November (4)) (2004) 1733–1741.
[11] H. Sun, Q. Guo, B. Zhang, et al., An adaptive zone-division-based automatic voltage control system with applications in China, IEEE Transactions on Power Systems 28 (2) (2013) 1816–1828.
[12] Q. Guo, H. Sun, M. Zhang, J. Tong, B. Zhang, B. Wang, Optimal voltage control of PJM smart transmission grid: study, implementation, and evaluation, IEEE Transactions on Smart Grid 4 (3) (2013) 1665–1674.
[13] F. Li, W. Qiao, H. Sun, H. Wan, J. Wang, Y. Xia, Z. Xu, P. Zhang, Smart transmission grid: vision and framework, IEEE Transactions on Smart Grid 1 (2) (2010) 168–177.
[14] K. Torchyan, M.S. Elmoursi, W. Xiao, Adaptive secondary voltage control for grid interface of large scale wind park, in: IEEE PowerTech Conference, Grenoble, France, 2013.
[15] Y. Liu, Z. Chen, Voltage sensitivity based reactive power control on VSC-HVDC in a wind farm connected hybrid multi-infeed HVDC system, in: IEEE PowerTech Conference, Grenoble, France, 2013.
[16] H. Eric, K. Dmitry, D. Matt, Wind hub reactive resource coordination and voltage control study by sequence power flow, in: IEEE Power and Energy Society General Meeting, Vancouver, Canada, 2013.
[17] T. Zheng, S. Jiao, K. Ding, L. Lin, A coordinated voltage control strategy of wind farms based on sensitivity method, IEEE PowerTech Conference, Grenoble, France, 2013.
[18] B. Zhang, H. Zhang, H. Sun, et al., Interaction and coordination between multiple control centers: development and practice, in: CIGRE 2006, SC C2 System Control and Operation, SC C2-302, 2006.
[19] H. Sun, B. Zhang, W.C. Wu, Q. Guo, Family of energy management system for smart grid, in: IEEE PES Innovative Smart Grid Technologies Europe, Berlin, Germany, October 13–18, 2012.
[20] Q. Guo, H. Sun, Y. Liu, et al., Distributed automatic voltage control framework for large-scale wind integration in China, in: IEEE Power and Energy Society General Meeting, San Diego, USA, 2012.
[21] Y. Li, J.D. McCalley, Decomposed SCOPF for improving efficiency, IEEE Transactions on Power Systems 24 (1) (2009) 494–495.

Please cite this article in press as: Q. Guo, et al., Hierarchical automatic voltage control for integration of large-scale wind power: Design and implementation, Electr. Power Syst. Res. (2014), http://dx.doi.org/10.1016/j.epsr.2014.02.012